JOURNAL OF MATERIALS SCIENCE 19 (1984) 1349–1358

Neutron and X-ray diffraction studies on pure and magnesia-doped zirconia gels decomposed in vacuo

N. H. BRETT, M. GONZALEZ*
Department of Ceramics, Glasses and Polymers, The University of Sheffield, UK

J. BOUILLOT
Institute Laue-Langevin, Grenoble, France

J. C. NIEPCE
University of Dijon, France

Pure and MgO-doped zirconia gels have been decomposed in vacuo at temperatures up to 800° C in a furnace attachment to the D1B neutron spectrometer at Institute Laue-Langevin (ILL). The recorded neutron line profile data were analysed to obtain a measure of the crystallite size of the product phase and the growth of the crystallites with increasing temperature; phase changes occurring during heating were also monitored. Additionally, the gel powders were decomposed *in situ* in a high temperature attachment to a Philips diffractometer and X-ray diffraction traces were obtained during progressive heating of the samples and after thermal cycling over a range of temperatures. The peak profiles were analysed to provide both crystallite size and strain values in the decomposed powders. The crystallite size values obtained from the two studies are compared with those obtained from a parallel small angle neutron scattering (SANS) study of the same gels after calcination.

1. Introduction

The improvement in the control and economics of fabrication methods brought about the by the development of sol–gel routes has promoted interest in the ceramic and chemical industries [1]. Notably, lower firing temperatures ensue from using gels rather than crystalline materials with a consequential saving in energy, particularly in the case of refractories where high sintering temperatures are normally encountered. Zirconia, stabilized in its cubic form by the addition of 10 to 15 wt% lime or magnesia, is finding increased use in specialized applications in the steel industry where the drive for increased efficiency dictates the maintenance of higher operating temperatures, e.g. in continuous casting procedures. Recent studies [2] on partially stabilized zirconia (PSZ) have shown that dramatic increases in the strength or toughness of the material may be brought about by the formation of metastable phases and these have led to an interest in the toughening mechanism. Stevens [3] has reviewed the recent literature on second phase particle toughening in ceramics and discussed the potential applications of PSZ material. Controversy exists over the role of the low temperature metastable tetragonal phase formed in pure zirconia but the importance of both the crystallite size of the tetragonal phase and the presence of strain at domain boundaries is generally accepted [4].

This study attempts to follow the development and growth of crystalline phases during the decom-

*Present address: Departmento de Quimica Inorganica Universidad, Sevilla, Spain.

0022–2461/84 $03.00 + .12

position in vacuo of zirconia and magnesia-doped zirconia gels using both neutron and X-ray diffraction methods. Previous work on lime-doped zirconia gels suggested that low temperature calcines contained ~ 4 nm crystallites although a precise determination was not made [5]. MgO-doped zirconia calcines are likely to have similar crystallite sizes and the presence of strain in these crystallites may be expected. X-ray line profiles have been analysed to assess this strain and in order to determine the crystallite–strain relationships in the microcrystals.

2. Experimental details

2.1. Materials

Pure and MgO-doped zirconia gels were prepared by dripping together a solution of zirconyl oxychloride ($50\,g\,l^{-1}$) and a suitable alkali. The reaction vessel was contained in a water bath at 22° C and the reactants were stirred continuously whilst the pH was controlled at 10.3 ± 0.1. In the case of MgO-doped samples, $MgCl_2$ solution of appropriate concentration was added to the zirconyl oxychloride solution. The gel preparations were left to settle for 24 h then decanted and centrifuged after washing with distilled water. The washing and centrifuge procedure was repeated a number of times until the filtrate showed a negative reaction to $AgNO_3$. After a final wash with acetone (this avoids the formation of hard glassy lumps on drying) the gels were dried for 24 h at 1100° C, lightly crushed in an agate and stored in a desiccator until use. Five gel samples were prepared; samples A and B by a precipitation route that employed soda as alkali and containing 0 and 3.26 mol % MgO, respectively (referred to the calcined gel composition) and samples C, D and E prepared using ammonia and containing 0, 16.4 and 18.1 mol %, respectively. The MgO content of samples B, D and E was determined by atomic absorption spectrometry, the water content of the gels obtained by the ATG–DTG method was approximately 6 mol H_2O per mol ZrO_2. The main water loss occurred from room temperature (RT) to 100° C and the DTG curve showed a maximum at 60° C. Electron micrographs of the gel powders were taken on an Hitachi HU-11A electron microscope after drying and after calcination at 400° C in air.

2.2. Neutron diffraction procedures

Powdered gel samples were loaded into a niobium sample holder and located in a high temperature furnace attachment to the D1B neutron spectrometer at ILL, Grenoble. The sample temperature was progressively raised at ~ 50° C/1 h from room temperature to about 800° C whilst the neutron diffraction spectra ($\lambda = 0.25226$ nm) were simultaneously recorded over the range 35 to 113.5° 2θ. The time to record sufficient spectra was approximately 25 min for each run and the mean temperature of the run is quoted when reporting the data. The experiments were carried out under a vacuum of 10^{-4} torr and pressure and temperature were recorded. Additionally, one sample (A) was raised to temperature by step-wise increments and held overnight at 595° C to measure the growth of crystallites at that temperature.

The crystallite size of the nucleated tetragonal phase was measured by curve fitting to non-overlapping peak profiles assuming Gaussian shapes, namely 101 reflection at 24.9°, 110 at 29.3 and 102 at 36.7° 2θ. Half breadths corrected to integral breadths were inserted in the Scherrer equation using the appropriate shape factor [6] and assuming tetrahedral crystallites, after allowing for instrumental broadening by use of a resolution curve determined for the D1B instrument [7]. The lattice parameters of the tetragonal phase were computed from the diffraction data using a programme developed at ILL [8].

2.3. X-ray diffraction procedures

Three of the powdered gel samples (A, B and E) were decomposed under a vacuum of 10^{-3} torr in a Rikagu-Denki high temperature furnace attachment to a Philips diffractometer that employed Ni-filtered Cu$K\alpha$ radiation. The furnace temperature was raised to 300° C then increased 50° C each 24 h or thereabouts up to 800° C; the samples were scanned ($1/8°\ 2\theta\ min^{-1}$) periodically over the range 27 to 34° 2θ to record the 101 diffraction trace. In a separate series of experiments samples were cooled from the holding temperature to room temperature then brought back to temperature and the profile remeasured, in order to assess the effect of thermal cycling on the strain in crystallites. Half-peak breadths were measured, corrected for α_2 broadening using the method [9] of Jones and converted to integral breadths (B) assuming Gaussian profile shapes from which the pure diffraction broadening (β) was obtained from the Warren relationship $\beta^2 = B^2 - b^2$, where b is the instrumental broadening determined from an

TABLE I Temperature of initial phase formation, lattice parameters and crystallite size of the tetragonal phase

Sample	Temperature range (°C)	Lattice parameters (nm)		Crystallite size (nm)			Particle diameter (nm) From SANS data [13]
		a	c	From 1 0 1	From 1 1 0	From 1 0 2	
A	300–312	0.3638	0.5230	8.23	–	–	7.06
B	308–327	0.3618	0.5257	8.37	9.61	–	7.18
C	275–289	0.3633	0.5241	–	10.73	6.63	8.41
D	458–474	0.3600	0.5220	11.80	–	–	4.88

Akansas stone (quartz) standard. The apparent crystallite size (ϵ) was determined from the Scherrer equation again assembling tetrahedrally shaped crystallites.

The method above employed to analyse peak profiles makes no allowance for strain which may be present in the crystallites and thus contribute to profile broadening. Therefore, the variance method was used to analyse the 101 diffraction profile (intensities were obtained from the peak profiles at 0.05°(2θ) intervals) to give comparative size and strain values by employing a computer program to calculate the variance-range function $W(2\theta)$ of the profiles [10]. Crystallite size and strain (e) were calculated from the slope and intercept given by [11]

$$W_{2\theta} = \frac{K\lambda}{2\pi^2}\frac{\Delta(2\theta)}{\epsilon\cos\theta} - \frac{L\lambda^2}{4\pi^2\epsilon^2\cos^2\theta} + 4\tan^2\theta\langle e^2\rangle$$

where K is the variance shape factor and L the taper parameter for crystallites assumed to be tetrahedral in shape [6]. The slope was corrected for spectral abberration when CuK X-radiation is used after the method of Edwards and Langford [12].

3. Results and discussion

3.1. Neutron diffraction studies

The results of the dynamic heating runs are first reported. In the four samples examined no diffraction lines were recorded (other than those of the furnace sample holder-niobium) until, at a critical temperature, an exothermic reaction was recorded accompanied by an abrupt pressure increase that resulted in a pressure peak on the pressure trace. Simultaneously, weak diffraction lines that corresponded to the tetragonal phase of ZrO_2 appeared and these grew in intensity with increasing temperature. The temperature of initial phase formation, the initial crystallite size determined from non-overlapping peak profiles and calculated lattice parameters are listed in Table I. Omissions in the table are where the profile was too weak or unreliable in shape to give confidence in the analysis. For comparison, the particle diameters obtained in a parallel SANS study, carried out on the same powders after calcination at 400° C for 2 h in air [13], are included in the table. The diffraction traces of one sample (D) obtained at a series of temperatures (dynamic heating) are shown in Fig. 1. The monoclinic phase was not formed at temperatures below 800° C; at room temperature after cooling all samples were shown by X-ray analysis to be composed of mixtures of tetragonal and monoclinic phases. Electron micrographs of the as-prepared gel powders revealed no discernable structure but the calcined powders were seen to be composed of aggregates of microcrystallites of sizes of the order of those determined by profile analysis, Figs. 2a and b.

The growth of crystallites with increasing temperature is shown in Fig. 3; the crystallite size values were derived from the 101 reflection except for sample C, for which the 102 peak data were used. Little change in crystallite size occurred up to 500 to 600° C for the pure zirconia samples (A and C) which then grew rapidly with increasing temperature. This was confirmed by a separate firing of sample A which was raised incrementally to 595° C and held overnight at that temperature; the crystallite size determined from the 101 peak increased from 10.46 to 19.7 nm. The presence of MgO in the gel retarded growth until about 700° C for sample B (3.26 mol % MgO) and 800° C for sample D (16.4 mol % MgO).

4.2. X-ray diffraction studies

Crystallite size as a function of calcination temperature was determined for three samples (A, B and E) from the measured half-peak broadening of the 101 diffraction profile, Fig. 4. The gel powders transformed to the metastable tetragonal phase at

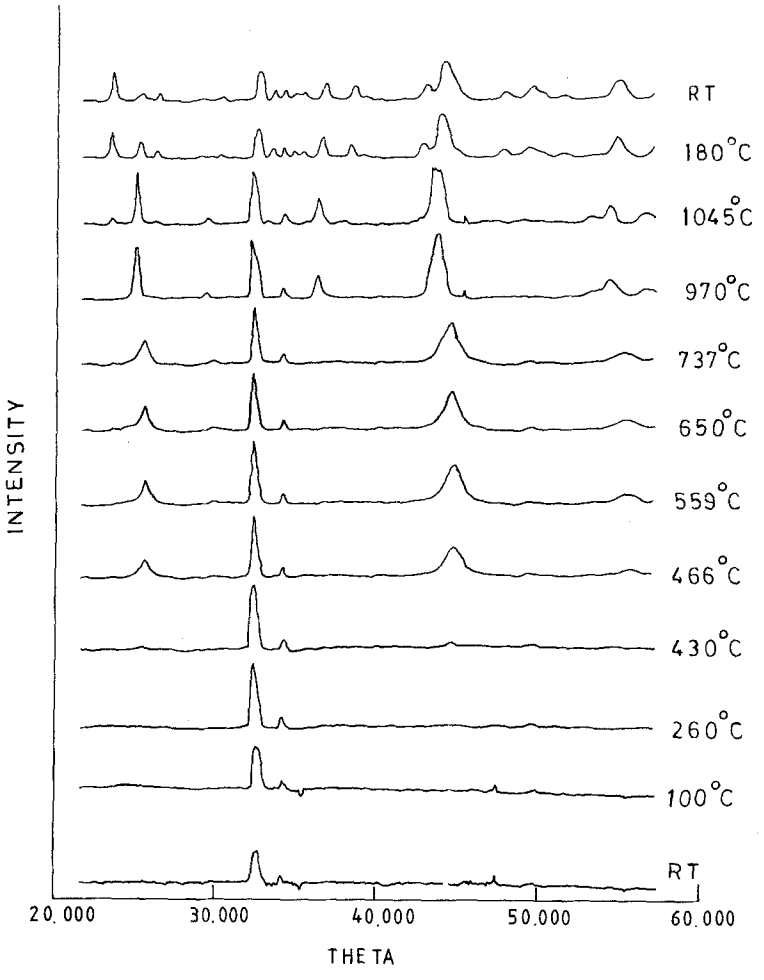

Figure 1 Neutron diffraction traces of Sample D (16.4 mol% MgO) at a series of temperatures.

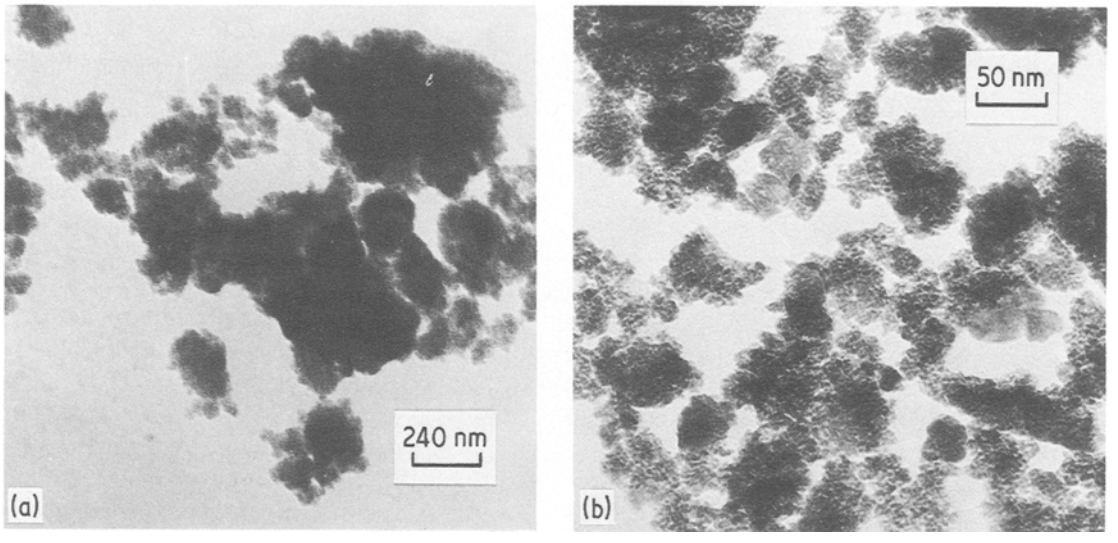

Figure 2 Electron micrographs of sample B (3.26 mol% MgO) (a) as-dried gel powder; (b) after calcination at 400° C in air.

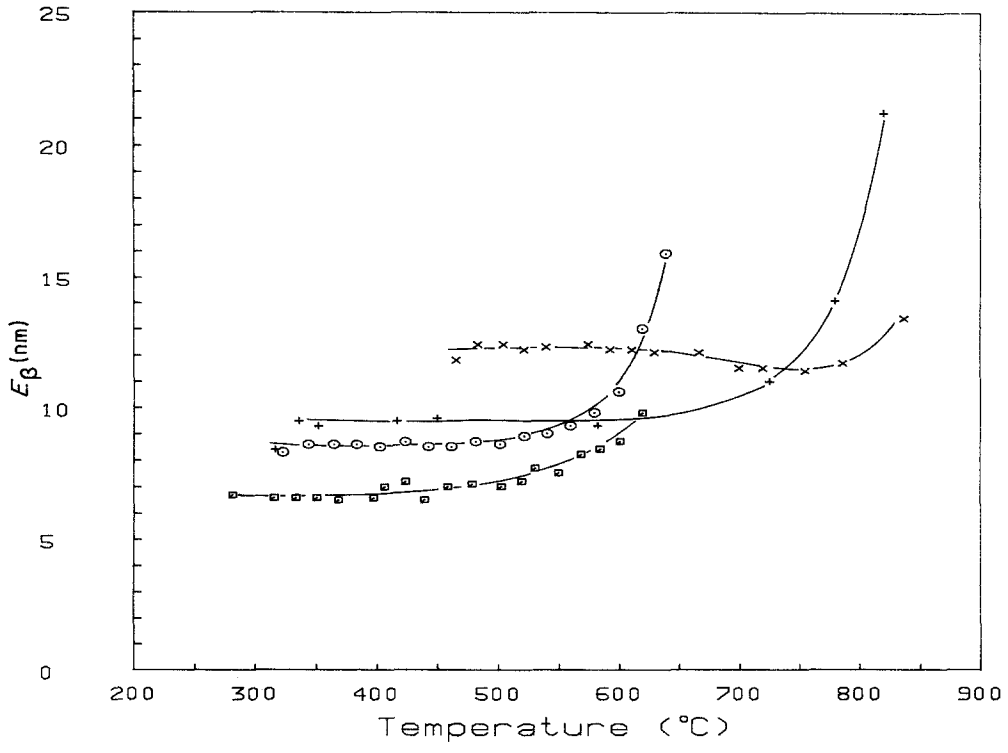

Figure 3 Crystallite size against temperature plots for neutron diffraction data: ⊙–Sample A (pure ZrO_2), ×–Sample B (3.62 mol% MgO), +–Sample C (pure ZrO_2), ⊡–Sample D (16.4 mol% MgO).

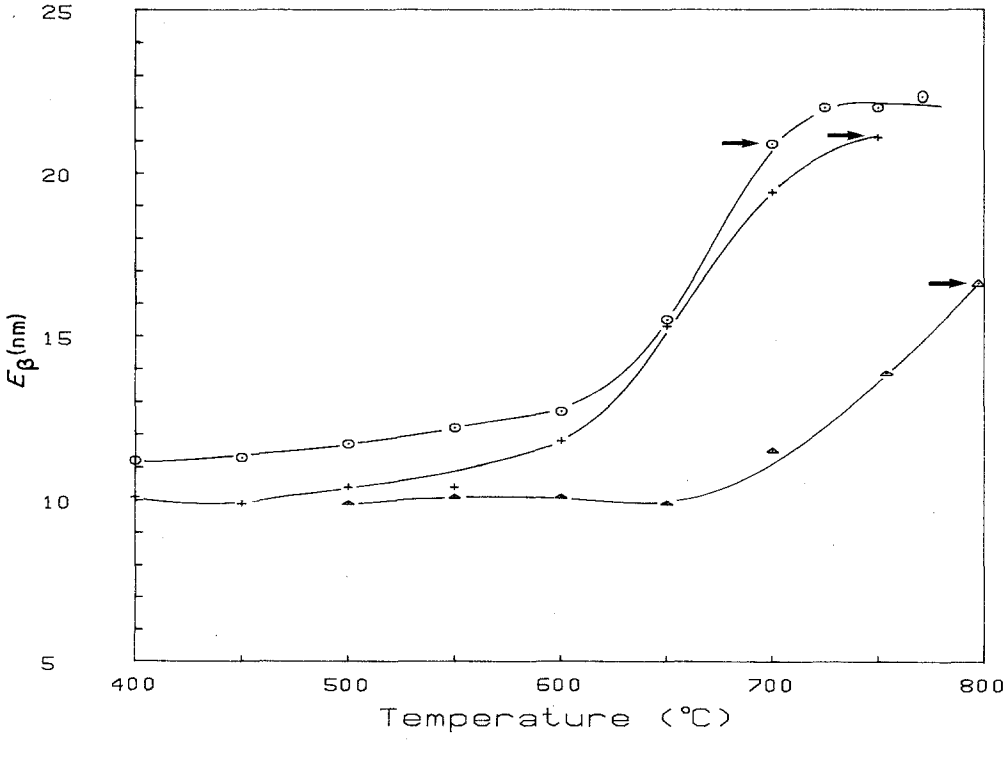

Figure 4 Crystallite size against temperature plots for X-ray diffraction data: ⊙–Sample A (pure ZrO_2), ×–Sample B (3.62 mol% MgO), ▲–Sample E (18.1 mol% MgO).

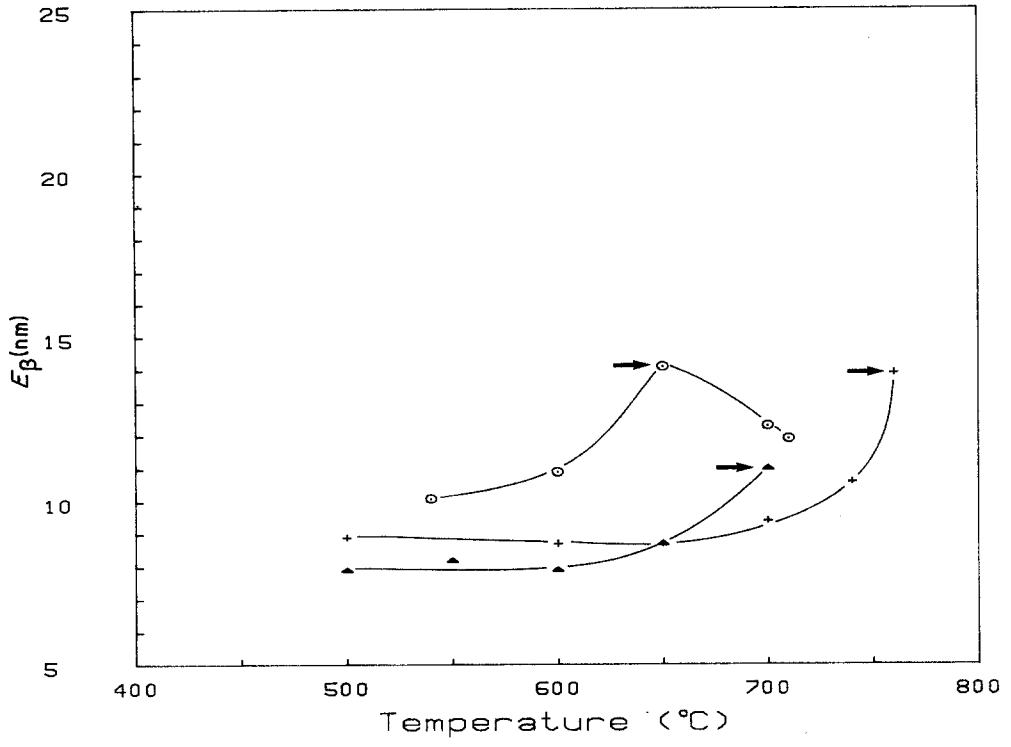

Figure 5 Crystallite size as a function of temperature after thermal cycling: ⊙–Sample A, X–Sample B, ▲–Sample E.

a temperature which increased with their magnesia content, as predicted by Polezhaev [14] and the present neutron diffraction studies. The presence of magnesia retards both the crystal growth and the temperature at which the stable monoclinic phase appears (arrowed in Fig. 4 and subsequent figures where appropriate). Complete transformation to the monoclinic phase did not occur after 24 h at the maximum temperature reached, namely, 750 to 800° C. After air was accidently admitted into the furnace into the furnace during one run with sample E (18.1 mol% MgO) it was observed that transformation to the monoclinic phase occurred at a higher temperature than under vacuum in agreement with Torralvo *et al.* [15].

Thermal cycling of the powders under vacuum resulted in lower crystallite sizes at a given temperature, probably due to the damage introduced in the samples and the temperature at which the monoclinic phase appears is modified, Fig. 5. In an attempt to measure the strain present in the microcrystallites the variance method was used to analyse the 101 peak profiles (see Section 2.3). Lower values of crystallite size were obtained from the variance analysis (Fig. 6) but the reduction in crystallite size due to thermal cycling the powders was confirmed, (Fig. 7). The strain values obtained from the analysis are shown in Fig. 8; strain increases to a maximum with increasing temperature then decreases with further increase in temperature over the range where crystal growth takes place. The effect of thermal cycling on strain values is shown in Fig. 9; strain is increased and higher values were found with increasing MgO content of the gels. The values of strain found in this work are regarded as comparative rather than accurate measures since only the 101 profile could be used in the analysis. They do, however, clearly demonstrate the inverse relationship between crystallite size and strain in the powders, Figs. 10 and 11.

4. Further discussion

The nucleation of the tetragonal phase in zirconia and magnesia-doped zirconia gels appears to take place quite suddenly on heating with the evolution of residual water at a temperature which is dependent on their MgO content. The crystallite size of the product phase is small, 5 to 10 nm, and growth is slow below 500° C but becomes significant above 600° C for the pure zirconia powders and above 700° C for the MgO-doped powders. The size values

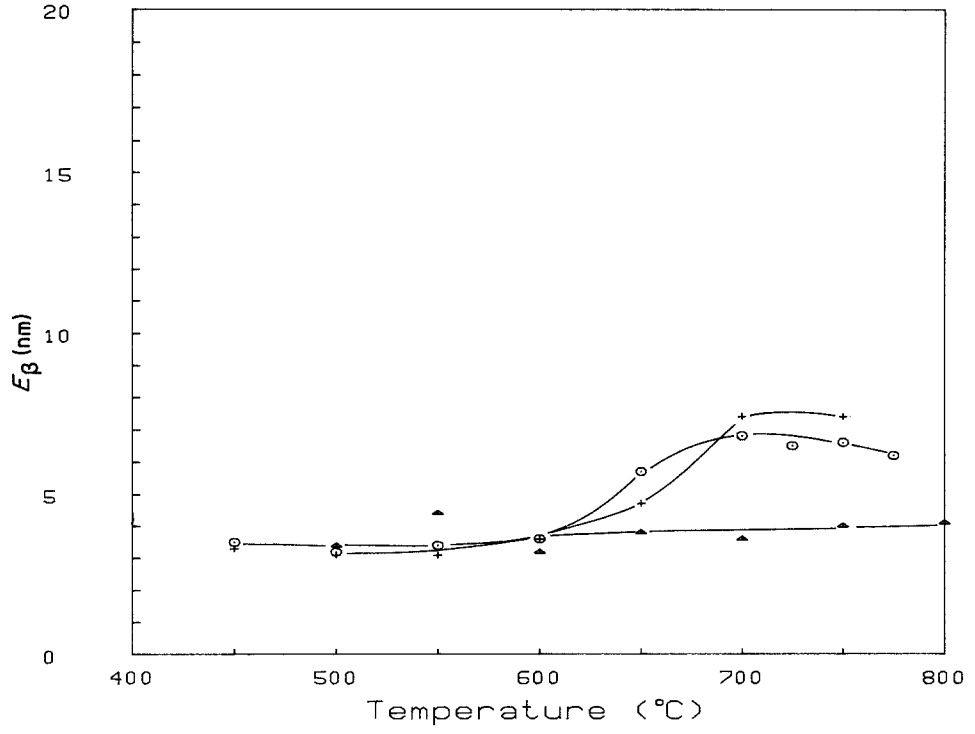

Figure 6 Crystallite size, obtained from variance analysis of profiles, as a function of temperature: ⊙–Sample A, ×–Sample B, △–Sample E.

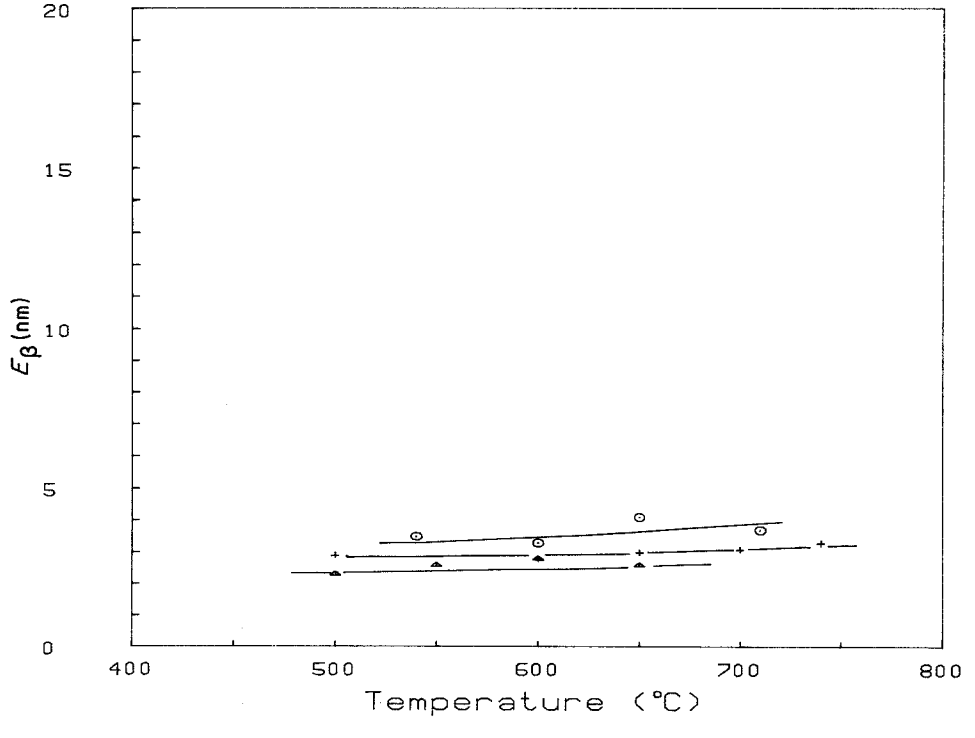

Figure 7 Crystallite size, obtained from variance analysis of profiles, as a function of temperature after thermal cycling.

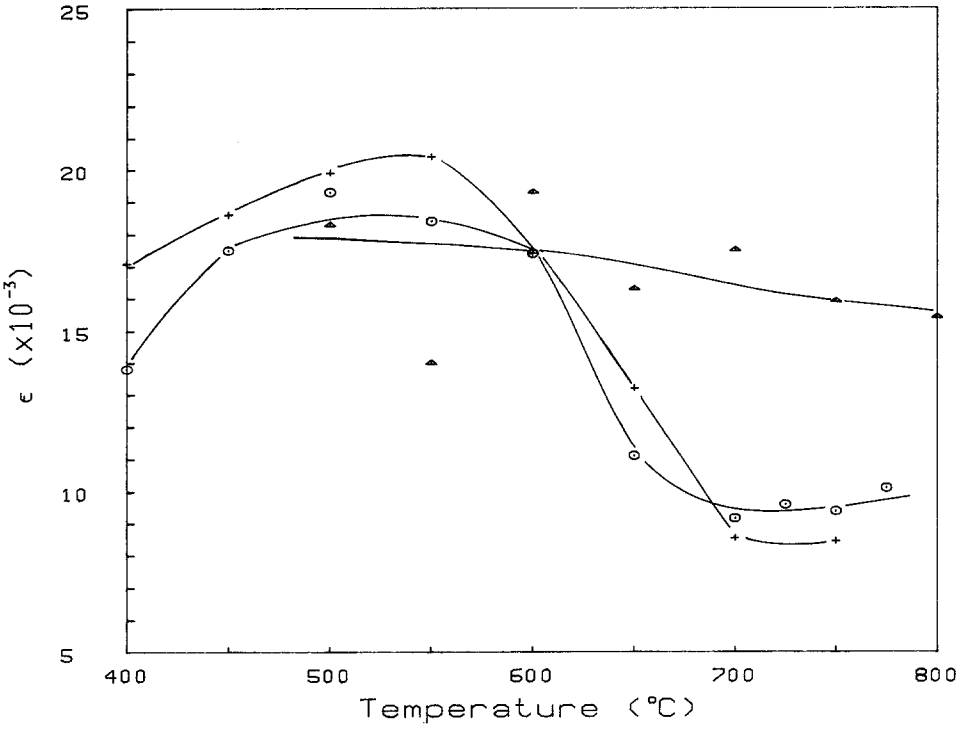

Figure 8 Values of strain, obtained from variance analysis of profiles, as a function of temperature: ⊙–Sample A, ×–Sample B, △–Sample E.

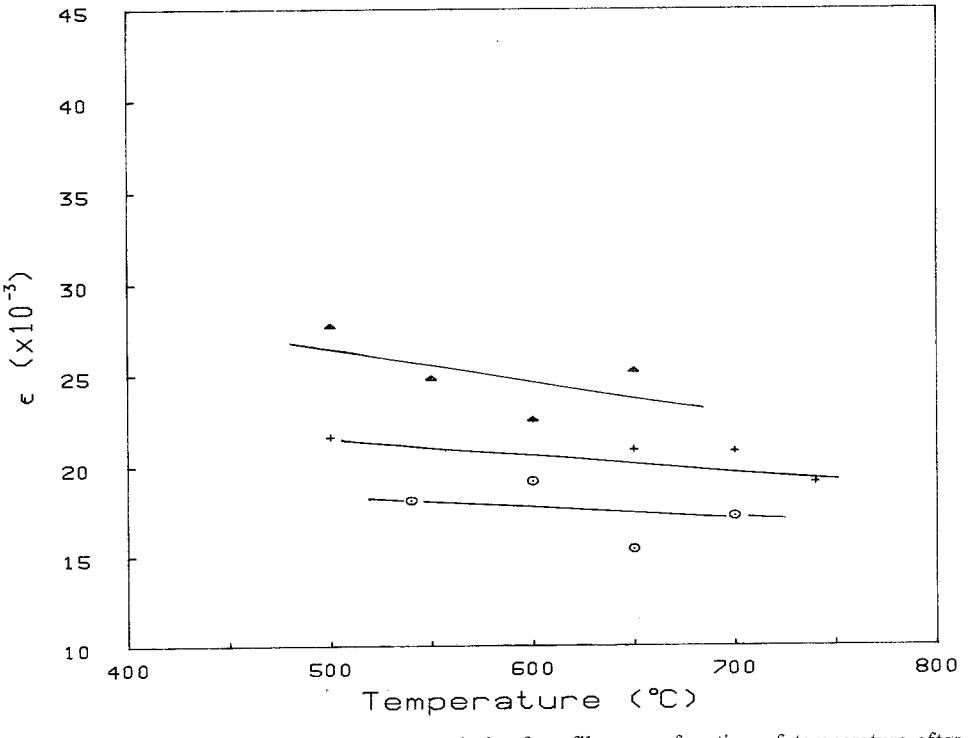

Figure 9 Values of strain, obtained from variance analysis of profiles, as a function of temperature after thermal cycling: ⊙–Sample A, ×–Sample B, △–Sample E. The black points correspond to strains measured at room temperature after cooling.

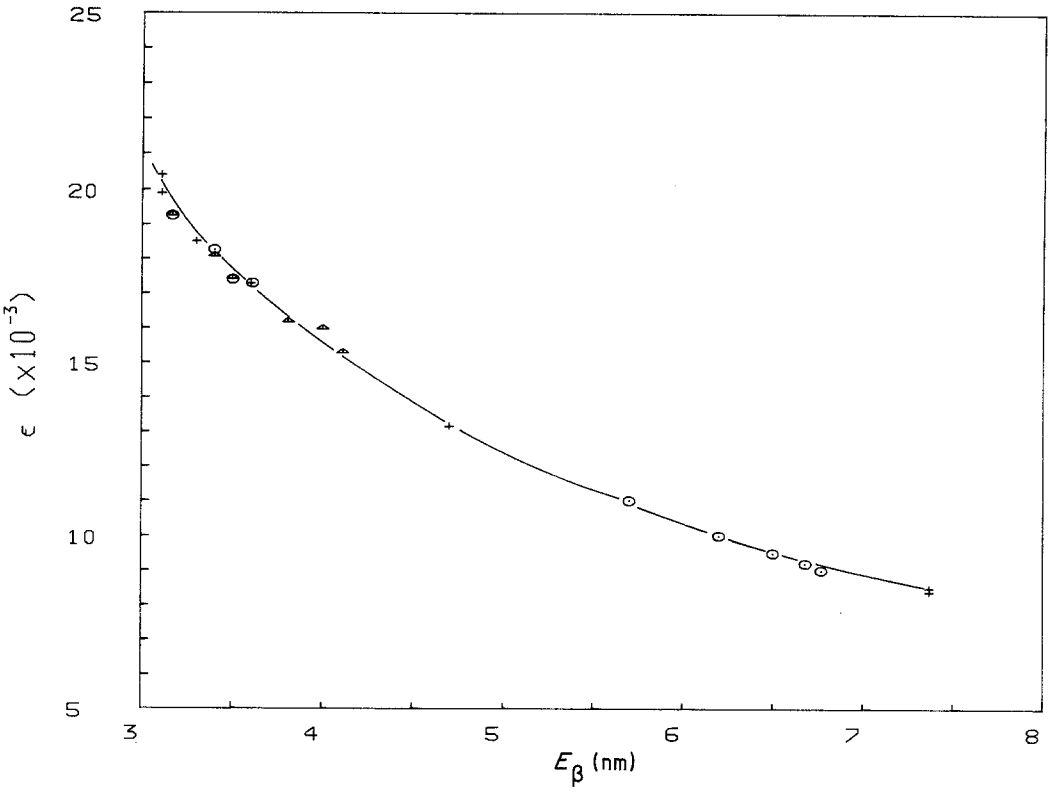

Figure 10 A plot of strain against crystallite size, values from variance analysis of profiles: ⊙–Sample A, X–Sample B, △–Sample E.

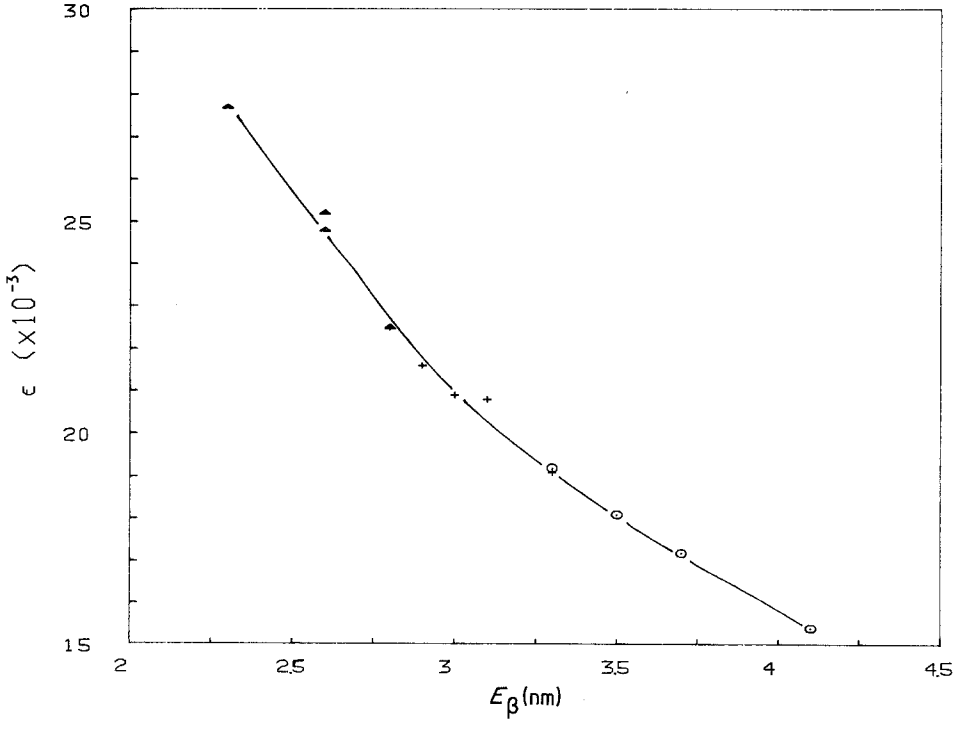

Figure 11 A plot of strain against crystallite size after thermal cycling, values obtained from variance analysis of profiles: ⊙–Sample A, X–Sample B, △–Sample E.

determined from the neutron and X-ray studies by assuming Gaussian profile shapes are in good agreement but may be high since all of the profile broadening is ascribed to the size effect and none to the presence of strain. In fact, analysis for strain by this method was not possible since too few non-overlapping profiles are present to permit Hall plots to be made. Variance analysis clearly shows that strain is present in the crystallites and lower crystallite sizes were found. It is interesting to note that the particle diameters determined by small angle neutron scattering were intermediate in value, Table I. Garvie [4], in his review on the stabilization of the tetragonal structure in zirconia microcrystals, calculates a critical size for monoclinic zirconia from thermodynamic considerations assuming spherical particles. The value found, 15.3 nm (or 153 Å) was lower than that quoted by other workers (~ 90 nm) for tetragonal precipitates found in thin films in partially stabilized zirconia and it was argued that the matrix imposes constraints on the transforming particle and that the transformation had to be nucleated. The work reported here supports this hypothesis, from Fig. 4 it can be seen that the first appearance of monoclinic phase occurs when the crystallite size value is 15 to 20 nm (or about 7 to 10 nm from variance analysis, Fig. 6). Moreover, the presence of MgO in the gel powders increases the strain, Fig. 10, and retards the transformation to monoclinic zirconia. In a bulk material, larger tetragonal precipitates may be expected since the restraining effect of the matrix will be greater than in microcrystalline powders.

References

1. J. L. WOODHEAD, "Science of Ceramics" Vol. 4 (British Ceramics Society, Stoke-on-Trent, 1968) p. 105.
2. R. C. GARVIE, R. H. HANNINK and R. T. PASCOE, *Nature* **258** (1975) 703.
3. R. STEVENS, *Trans, J. Brit. Ceram. Soc.* **80** (1981) 81.
4. R. C. GARVIE, *J. Phys. Chem.* **82** (1978) 218.
5. I. F. GUILLIATT and N. H. BRETT, *J. Mater. Sci.* **9** (1974) 2067.
6. J. I. LANGFORD and A. J. C. WILSON, *J. Appl. Cryst.* **11** (1978) 102.
7. M. PANNETIER, I.L.L. Grenoble, private communication (1982).
8. J. BOUILLOT, I.L.L. Grenoble, private communication (1982).
9. F. W. JONES, *Proc. Roy. Soc. (Lond.)* **A166** (1938) 16.
10. H. J. EDWARDS and K. TOMAN, *J. Appl. Cryst.* **2** (1969) 240.
11. H. P. KLUG and L. E. ALEXANDER, "X-ray Diffraction Procedures for Polycrystalline and Amorphous Materials" (John Wiley and Sons, New York, 1974) p. 660.
12. H. J. EDWARDS and J. I. LANGFORD, *J. Appl. Cryst.* **4** (1971) 43.
13. A. F. WRIGHT, P. W. McMILLAN and N. H. BRETT, "The Structure of Non-Crystalline Materials 1982", edited by P. H. Gaskell, J. M. Parker and E. A. Davis (Taylor and Francis Ltd., London, 1983) p. 569.
14. Yu. M. POLEZHAEV, *Russ. J. Phys. Chem.* **41** (1967) 1590.
15. M. J. TORRALVO, J. SORIA and M. A. ALARIO, 9th International Symposium on Reaction of Solids, Cracow, 1980 (Elsevier, New York, 1980) p. 512–16.

Received 27 July
and accepted 29 July 1983